nature nanotechnology

SUPPLEMENTARY INFORMATION

DOI: 10.1038/NNANO.2015.23

Plateau–Rayleigh crystal growth of periodic shells on one-dimensional substrates

Robert W. Day, Max N. Mankin, Ruixuan Gao, You-Shin No, Sun-Kyung Kim, David C. Bell, Hong-Gyu Park* and Charles M. Lieber*

*email: hgpark@korea.ac.kr; cml@cmliris.harvard.edu

Materials and Methods

Periodic Shell Nanowire Synthesis. *Si periodic shell nanowire growth:* Au nanoparticle catalysts (20, 30, 50, 80, and 100 nm; Ted Pella) were diluted 1 to 100 by volume in water and subsequently dispersed on an oxidized Si growth chip (p-type Si, 0.005 Ω cm, 600 nm oxide; Nova Electronic Materials) functionalized with 0.1% w/v poly-L-lysine (150,000 – 300,000 g/mol; Sigma Aldrich) in water. After rinsing in deionized water and drying with nitrogen, the substrates were placed into a home-built chemical vapour deposition reactor and the system was evacuated to a base pressure of ~5 mTorr. Si core nanowires were grown via the Au nanoparticle catalysed growth mechanism[S1] for ~10-60 minutes at 465°C and a total pressure of 40 Torr with 1 standard cubic centimetre per second (sccm) silane (SiH_4; 100%; Voltaix) and 60 sccm hydrogen (H_2; 99.999%; Matheson) flow rates. Following core growth, the furnace temperature was ramped to 700-850°C for shell growth. At this temperature, shells were grown for 1-60 minutes at ~0.3 Torr with gas flow rates of 0.15-10 sccm SiH_4 and 0-200 sccm H_2. For some syntheses, phosphine (PH_3, 1000 p.p.m. in H_2; Voltaix) was introduced to the reactor during shell growth at 0.5-20 sccm flow rates. *Ge periodic shell nanowire growth:* Germanium core nanowires were typically synthesized from 50 nm Au nanoparticle catalysts at a total pressure of 300 Torr with 200 sccm H_2 and 20 sccm germane (GeH_4; 10% in H_2; Voltaix) flow rates. Ge cores were nucleated for 5 minutes at 330°C and grown for another 50 minutes at 270°C. For heterostructure growth, Si cores were grown in the same way as described for Si shells on Si cores. Ge periodic shells were grown on the Si cores by increasing the temperature to 450 – 600°C and decreasing the pressure to ~0.3 Torr with GeH_4 flow rates of 1-40 sccm.

Nanowire Characterization. End-on view scanning electron microscopy (SEM, Zeiss Ultra Plus field emission SEM) images of periodic shell nanowires were recorded directly from the as-synthesized growth wafers. For plan-view SEM images and nanowire pitch measurements, nanowires were transferred to Si_3N_4-coated Si wafers (200 nm Si_3N_4, 100 nm SiO_2 on p-type Si, 0.005 Ω cm; Nova Electronic Materials). Transmission electron microscopy (TEM) and diffraction samples were prepared by shear transfer methodology[S2] on amorphous carbon-coated copper TEM grids. The samples were imaged directly in JEOL 2100 or JEOL 2010F field emission high resolution TEMs operating at 200 keV. High-angle annular dark-field scanning TEM (HAADF-STEM) imaging and analysis was performed on an aberration corrected Zeiss Libra 200 MC operating at 200 keV. Energy dispersive X-ray spectroscopy (EDS) maps were collected at 512 x 400 resolution using a 400 ms dwell time per pixel in commercial EDAX Genesis software. Optical dark field images of nanowires on silicon nitride-coated substrates were recorded using an Olympus BX51 microscope.

Relative stability of periodic shell nanowires. To obtain a qualitative understanding of the stability of different periodic shell structures, we have compared the surface areas of different 1D configurations. We assume that surface energies of nanowires can be approximated by their surface areas[S3,S4]. The periodic shell nanowires were modelled as adjoining cylinders of lengths L_{inner} and L_{outer} and diameters D_{inner} and D_{outer}; one inner and one outer cylinder define a unit cell. We assume the additional volume is added, V_{added}, to the outer shell and that D_{inner} is unchanged and corresponds to the original diameter of the nanowire core:

$$V_{added} = V_{outer} - V_{core} = \frac{\pi L_{outer}}{4}({D_{outer}}^2 - {D_{core}}^2) \quad (1)$$

In Supplementary Fig. 10a, we consider the specific case in which V_{added} is constant and pitch is fixed at 3 μm but modulation amplitude is not fixed. V_{added} was obtained from dimensions of a typical periodic shell nanowire measured by SEM (L_{inner} = 1,500 nm, L_{outer} = 1,500 nm, D_{inner} = 100 nm, D_{outer} = 300 nm, and total length, L_{total}, = 30 μm). If this V_{added} were distributed uniformly along the nanowire axis, the nanowire would have a uniform diameter along its axis of

$$D_{straight,equiv} = \left(\frac{4(V_{added} + V_{core})}{\pi(L_{inner} + L_{outer})}\right)^{\frac{1}{2}} \quad (2)$$

For these dimensions, $D_{straight,\ equiv}$ = ~223.6 nm. The surface area of the periodic shell to the surface area of the straight nanowire is $SA_{Periodic}/SA_{straight,equiv}$.

We determine the surface areas of nanowires with different modulation amplitudes by varying L_{outer} (and thus $L_{inner,}$ since $L_{outer} + L_{inner}$ = pitch = 3,000 nm) for 20 nm < L_{outer} < 3,000 nm in increments of 20 nm. Since V_{added} is constant, D_{outer} must also change with L_{outer}. For every D_{outer}, we calculate the surface area. Absolute surface area values can be compared for a given D_{outer} or dimensionless comparisons can be made with ratios of periodic shell surface areas to straight nanowire surface areas for a given diameter modulation (where diameter modulation = D_{outer}/D_{inner}, and D_{inner} is constant here at 100 nm). See Supplementary Fig. 10a for additional calculations of surface area vs. diameter modulation with different values of V_{added}.

For consideration of surface area vs. pitch (Fig. 2c), we expand the above calculation by considering pitches ranging from 500 nm to 15 μm in increments of 100 nm; for the general case with different pitches, there are n = L_{total}/pitch unit cells per nanowire and the volume is distributed evenly among the n

outer shells. We perform the analysis for each pitch to produce surface areas as a function of diameter modulation and the minimum surface area for a given pitch is then plotted as a function of surface area vs. pitch. See Supplementary Fig. 10b for additional calculations of surface area vs. pitch with different values of V_{added}.

This simple geometric analysis is material-independent and dimensionless, and as expected, shows that periodic shell nanowires can have reduced surface energies compared to uniform diameter nanowires of equivalent volume.

We have also performed a similar analysis with the cross sectional morphologies and specific Si surface facets experimentally observed in periodic shell growth (Supplementary Fig. 10c). We use the same V_{added}, L_{inner}, L_{outer}, and pitch that we applied to the above cylindrical cross-section calculations. Then, we compute the surface energy for the periodic shell nanowires with experimentally observed cross sections (Supplementary Fig. 11) with a variety of diameter modulations and cross sectional aspect ratios and compare it to the surface energy of a uniform-diameter nanowire of equivalent volume and cross sectional aspect ratio. Surface energy (SE) is defined as $SE = \sum A_i \gamma_i$, where A_i is the area of surface i and γ_i is its surface energy density. We use surface energy densities of 88.6 and 94.8 meV/Å^2 for the Si{111} and {113} surfaces, respectively[S5]. The angles between facets were defined by the crystallographic properties of Si and closely match the angles between facets observed in end-on SEM images of faceted periodic shell nanowires (i.e. 60.5° and 119.5° between adjacent {113}/{113} and {111}/{113} facets, respectively). For the transitional facets (the crystal faces between the inner and outer shells), we assume the average surface energy of the {111} and {113} surfaces. Importantly, we find that the periodic shell nanowires with experimentally-observed cross sections have reduced surface energies compared to uniform diameter nanowires of equivalent volume and cross sectional aspect ratio. These results are similar to our calculations of relative stabilities (periodic shell vs. uniform) based on surface area analysis.

Estimation of diffusion lengths. For conditions similar to our experiments (i.e., SiH_4 partial pressures from ca. 1 to 40 mTorr, and temperature ranges from 735 to 855°C), Lim et al. estimate diffusion lengths of 70 nm, 140 nm, and 200 nm at 550, 600, and 650°C at SiH_4 partial pressures of 0.6 mTorr on the Si(100) surface[S6]. Given (1) that diffusion lengths increase exponentially with temperature (this holds true for temperatures < 900°C; for temperatures of 900-1000°C, diffusion lengths begin to decrease due to Si adatom desorption rates becoming appreciable), and (2) that diffusion lengths on Si (111) (i.e. our major surfaces) are approximately an order of magnitude higher compared to those on Si (100)[S7], we estimate a lower limit for diffusion lengths of >200 nm to 2000 nm for shell deposition at the lower regime of

temperatures used in our studies. Indeed, we begin to observe periodic shells with average pitch of 1.2 μm (Supplementary Fig. 8) at 735°C and a SiH_4 partial pressure of 14 mTorr on 100 nm cores.

For higher temperatures and lower pressures, we can expect an increase in diffusion lengths until desorption becomes appreciable at temperatures >900°C. We are unable to perform periodic shell growth experiments at temperatures greater than 900°C as the underlying nanowire cores transform into isolated particles very quickly due to the Plateau-Rayleigh instability, as shown in Fig. 1b. Although estimates for surface diffusion lengths of Si cannot be found for CVD deposition with SiH_4 at temperatures approaching 900°C, we estimate an upper limit of diffusion lengths using values reported from studies on annealed (i.e. no growth) Si(111) and Si(100) surfaces. At 900°C, Si diffusion lengths have been estimated up to 10s of microns[S8,S9]. This serves as an upper limit for our diffusion lengths at 855°C; that is, the diffusion length will be reduced for our growths due to incoming flux of SiH_4 molecules as well as lower temperatures.

In summary, we estimate diffusion lengths in the periodic shell growth regime to be > 200 nm at our lowest temperature of 735°C and 10s of microns at the highest temperature of 855°C used in our growth. This range encompasses the observed pitch range from our experiments (i.e. 500 nm to 10 μm).

Given that (1) our conservative lower limit of diffusion lengths suggests that diffusion lengths are on the order of our observed pitches, (2) that these diffusion lengths scale with temperature and pressure similarly to how periodic shell pitch scales with temperature and pressure, and (3) that it is known from literature that diffusion lengths are important factors for determining morphology at our CVD conditions using SiH_4[S3,S6], it is reasonable to conclude that surface diffusion lengths contribute significantly to formation of periodic shells.

Finite-Difference Time-Domain (FDTD) calculations. Analyses were performed using incident plane waves with the transverse-electric (TE) polarization state normal to a single nanowire/substrate. In the calculations, the nanowire and substrate parameters are consistent with experimental values (e.g. substrates are 200 nm thick Si_3N_4/100 nm thick SiO_2). The absorption cross section of a nanowire was calculated using periodic and perfectly matched layer boundary conditions[S10,S11]. For a periodic shell nanowire with a finite pitch, we divided the nanowire into small segments with lengths of 50 nm along the nanowire axis and calculated the absorption cross section at each segment (Fig. 4 and Supplementary Fig. 12). In the periodic shell nanowire simulations, calculations were performed with a spatial resolution of $10/\sqrt{3}$, 10, and 10 nm for each axis and a calculation domain size of $1.6/\sqrt{3}$ x 6 x 0.9 μm^3.

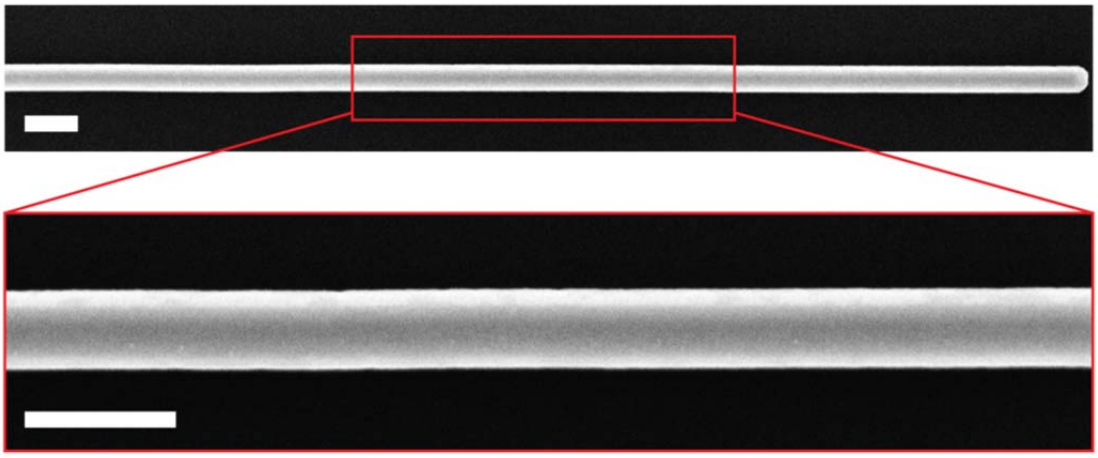

Supplementary Figure 1 | Annealed 100 nm Si cores. SEM images of a 100 nm Si core nanowire that was annealed at 775°C for 2 hours at ~ 0.3 Torr in hydrogen directly following core growth. Scale bars, 200 nm. We observe minimal rearrangement of 100 nm nanowire cores for times much longer (e.g. 2 hours) than periodic shell growth times (e.g. < 10 minutes), suggesting that traditional Plateau-Rayleigh instability does not drive rearrangement of the nanowire cores before or during growth of periodic shells.

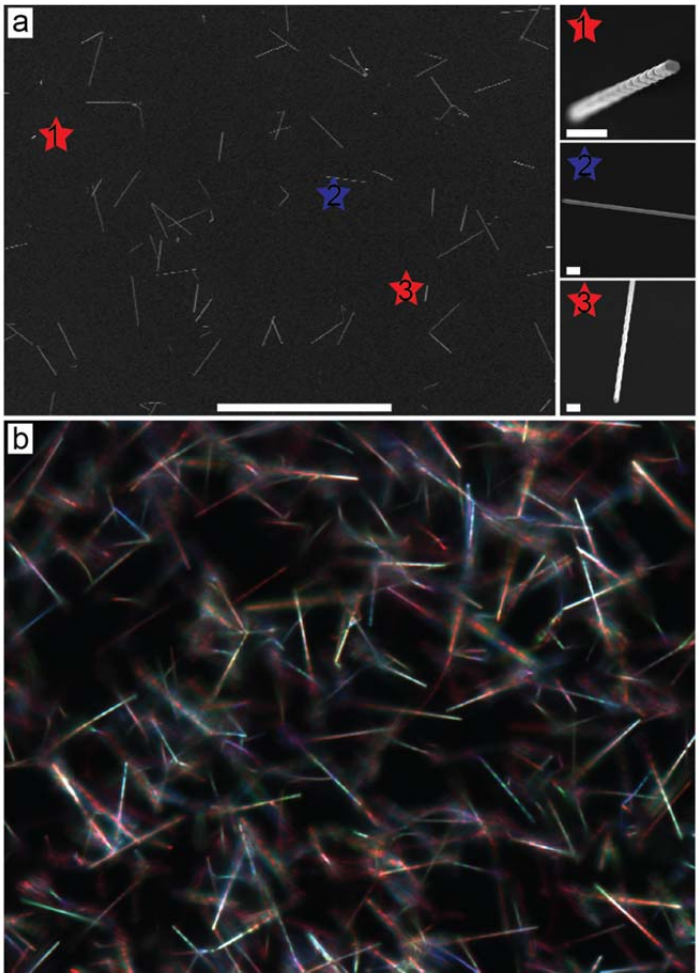

Supplementary Figure 2 | Yield of diameter-modulated nanowires. a, Left, SEM image of a ~300 x 250 μm^2 area from a periodic shell nanowire growth substrate. The nanowires were obtained from a synthesis in which Si shells were deposited onto 100 nm cores at 775°C with a SiH_4 flow rate/partial pressure of 3 sccm/15 mTorr at a total pressure of ~0.3 Torr for 3 minutes. Scale bar, 100 μm. Right, high resolution SEM images of the single nanowires denoted in the wide area image to the left. The red stars indicate representative images of nanowires that clearly have diameter modulations; the blue indicates a nanowire without clear diameter modulation from SEM imaging. Scale bars, 1 μm. Examining all of the nanowires in the large area region indicates that the yield of diameter-modulated nanowires is ~90%. **b,** Optical dark field image of a periodic shell nanowire growth substrate. The image was recorded using a 20x objective and an extra 1.6x magnifying lens; subsequently, the colour tone of the entire image was adjusted in Adobe Photoshop to reduce the background in order to provide the best contrast for the diameter-modulation of the nanowires to be visible.

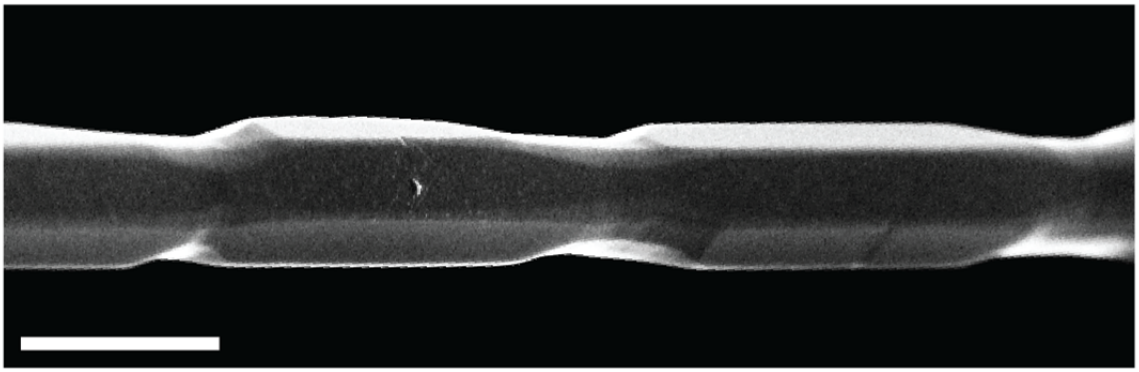

Supplementary Figure 3 | Periodic shell growth following removal of Au catalyst. SEM image of a representative Si periodic shell nanowire grown on a Si nanowire core whose Au catalyst was removed by a previously published procedure[S10] prior to P-R crystal growth. Briefly, immediately after the growth of 100 nm Si cores, the growth substrate was removed from the reactor and immersed in KI/I_2 solution for 2 minutes, followed by rinsing with deionized water, etching in buffered hydrofluoric acid (BHF) for 1 minute and rinsing in deionized water. Before drying, the substrate was immersed in liquid N_2 and placed into the reactor; the pressure was immediately lowered to ~0.1 Torr. The subsequent sublimation process prevents the collapse of nanowire cores via capillary action onto the growth substrate. When the reactor achieved base pressure, the temperature was increased to 775°C, followed by deposition of periodic shells under representative growth conditions; shells were grown for 3 minutes with a SiH_4 flow rate/partial pressure of 3 sccm/15 mTorr at a total pressure of ~0.3 Torr. Scale bar, 500 nm. Observed pitches of ~3-4 μm, inner diameters of ~300-400 nm, and outer diameters of ~400-500 nm are comparable to nanowires whose periodic shells were grown under the same conditions directly after core synthesis without removal of the Au catalyst (see Supplementary Fig. 7b). The lack of significant difference between shells grown on nanowires with or without Au indicates that Au does not contribute to the formation of periodic shells.

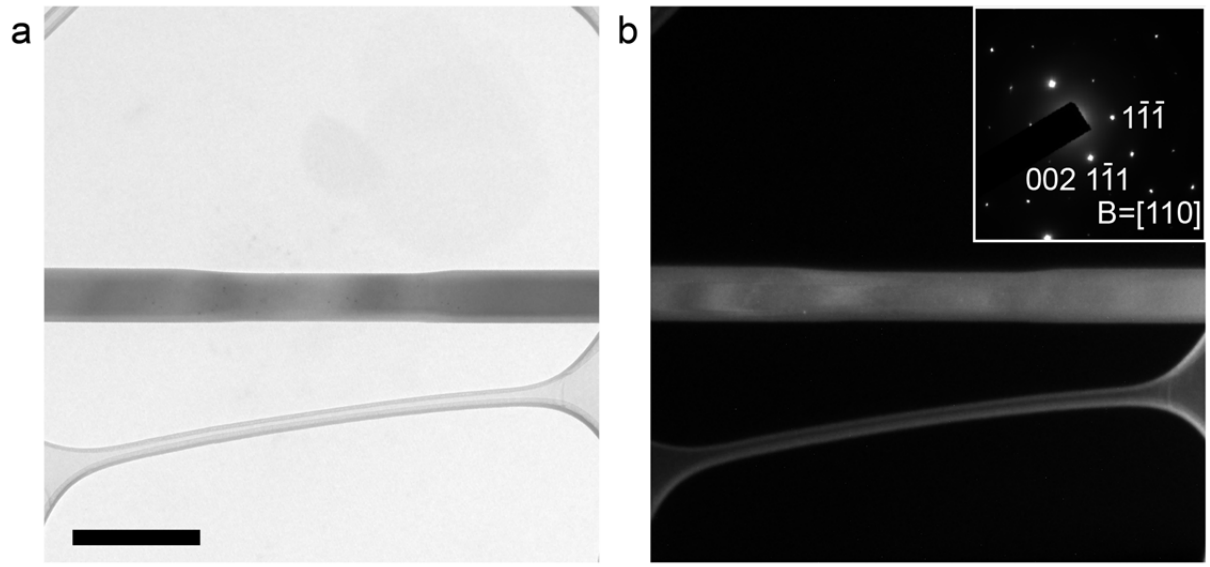

Supplementary Figure 4 | Crystallographic characterization of Si periodic shell nanowires in the [110] zone axis. a,b, Bright (**a**) and dark (**b**) field TEM images of a nanowire tilted to the [110] zone axis. Scale bar, 500 nm. The dark field TEM image was recorded using a (2-20) reflected beam. Inset, selected area electron diffraction patterns in the [110] zone axis. The alternating dark-light lines along the length of the nanowire stem from thickness fringes due to the thickness change between the inner and outer shells.

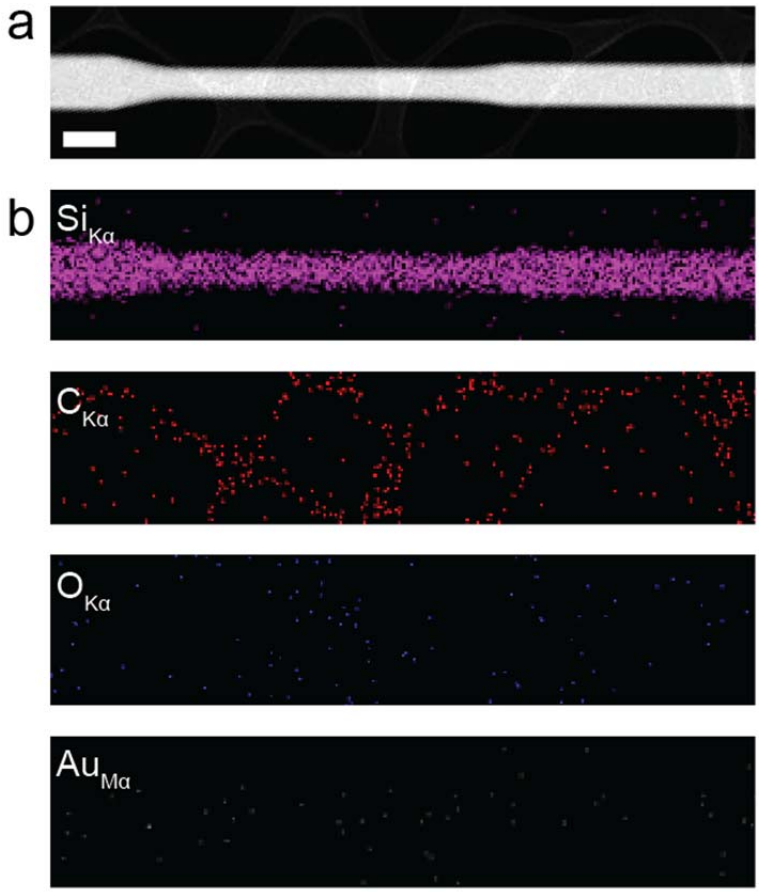

Supplementary Figure 5 | Elemental mapping of a Si periodic shell nanowire. a, A low magnification HAADF-STEM image of a typical periodic shell nanowire. Scale bar, 500 nm. **b,** EDS maps of Si, C, O, and Au from the same area shown in (**a**). X-ray counts from Si and C match the locations of the nanowire and the amorphous carbon film, respectively, whereas O and Au counts are comparable to background signal. Elemental analysis suggests that impurities do not contribute to periodic shell formation.

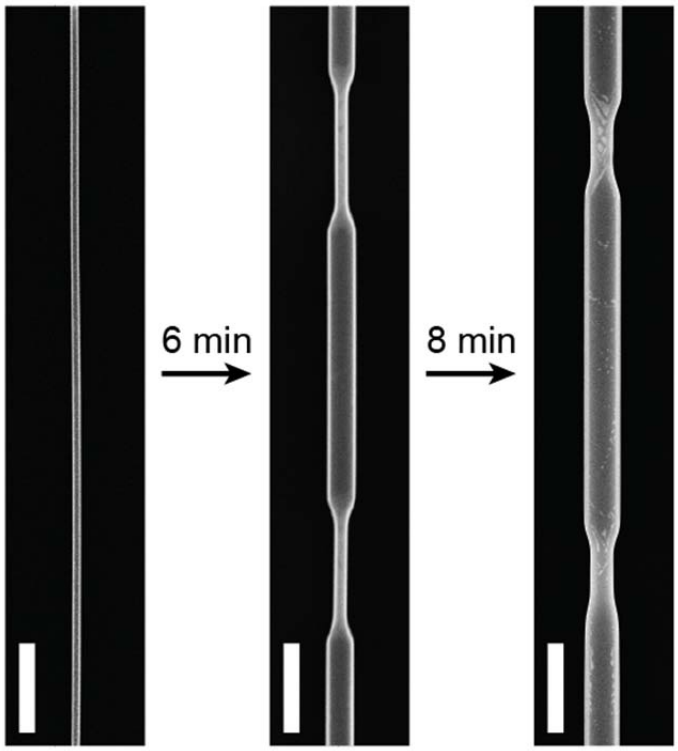

Supplementary Figure 6 | Time-sequence of periodic shell growth. SEM images of nanowires obtained from distinct syntheses for which Si shells were deposited onto 100 nm diameter cores at 800°C with a SiH_4 flow rate/partial pressure of 0.8 sccm/4 mTorr at a total pressure of ~0.3 Torr for 0 (left), 6 (middle), and 8 (right) minutes. Scale bars, 1 μm. The inner shell diameters of the nanowires in the middle and right images are 160 nm and 240 nm, respectively; the outer shell diameters of the nanowires in the middle and right images are 320 and 415 nm, respectively. The pitch of both nanowires is ~4.5 μm, demonstrating that pitch does not change with time.

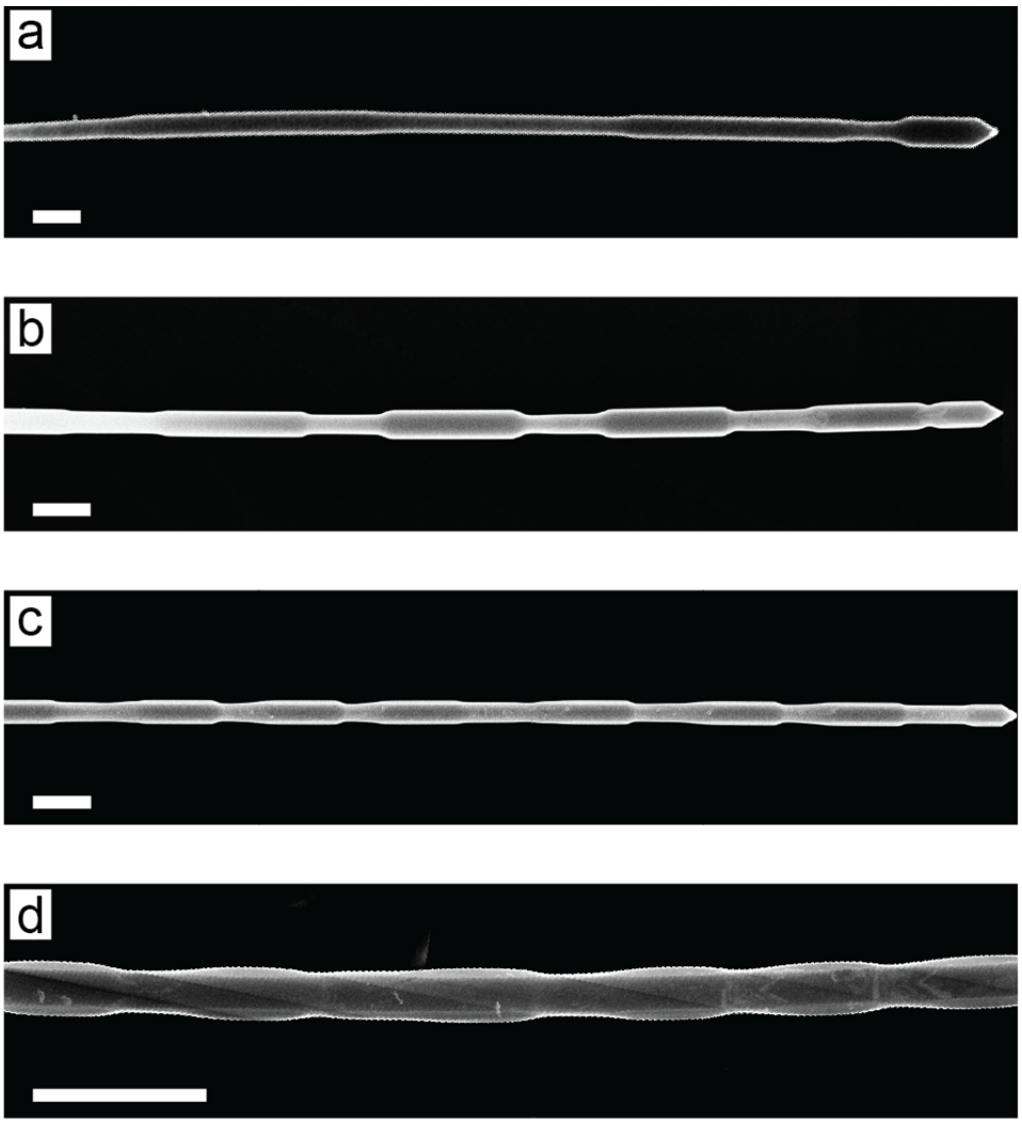

Supplementary Figure 7 | Pitch as a function of SiH_4 flow rate. Plan view SEM images of periodic shells grown on 100 nm cores at ~0.3 Torr total pressure and 775°C with (**a**) 0.3 sccm/1 mTorr, (**b**) 1 sccm/5 mTorr, (**c**) 3 sccm/15 mTorr, and (**d**) 9 sccm/47 mTorr SiH_4. Scale bars, 1 μm. These are representative nanowires whose pitches contributed to the data shown in Fig. 2a. Average pitches for (**a**), (**b**), (**c**), and (**d**) are 7.8, 3.8, 2.5, and 1.2 μm, respectively. Pitch is inversely proportional to SiH_4 flow rate. The diagonal lines in (**d**) are an artefact stemming from line scans of the SEM.

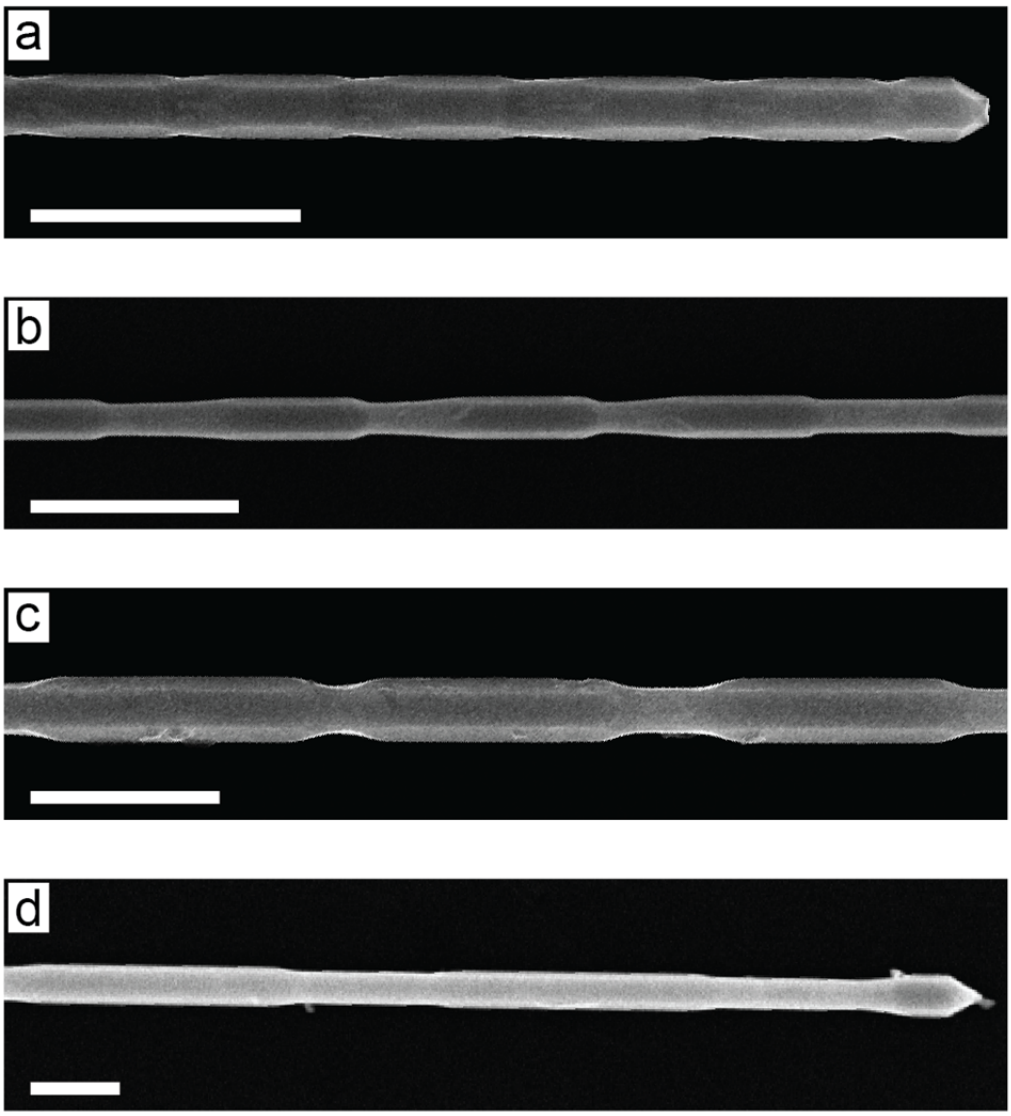

Supplementary Figure 8 | Pitch as a function of temperature. Plan view SEM images of periodic shells grown on 100 nm cores at ~0.3 Torr total pressure with 3 sccm/15 mTorr SiH_4 at (**a**) 735, (**b**) 775, (**c**) 815, and (**d**) 855°C. Scale bars, 2 μm. These are representative nanowires whose pitches contributed to the data shown in Fig. 2b. Average pitches for (**a**), (**b**), (**c**), and (**d**) are 1.2, 2.5, 4.0, and 8.3 μm, respectively. Pitch is proportional to periodic shell growth temperature.

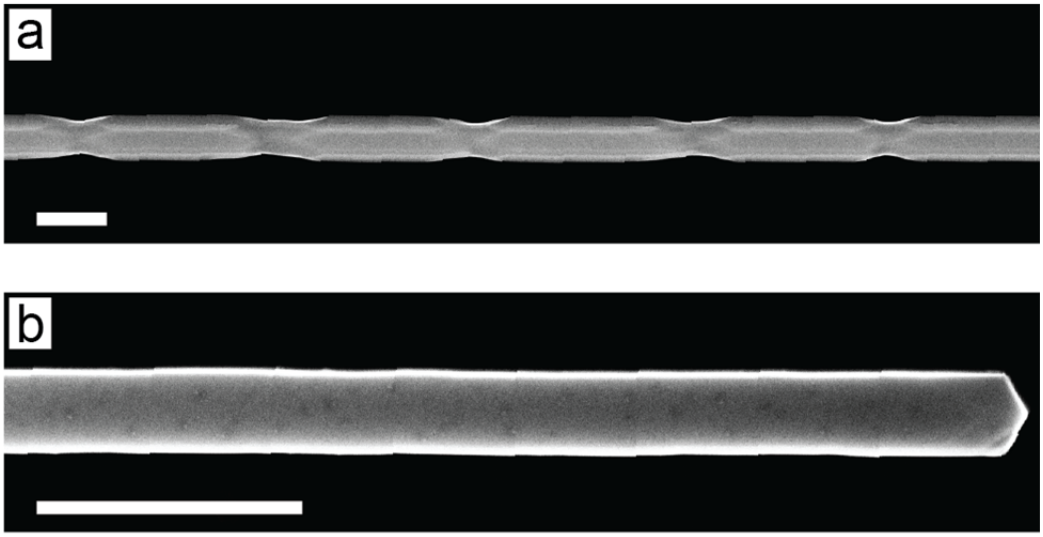

Supplementary Figure 9 | Pitch as a function of phosphine flow rate. Plan view SEM images of n-type periodic shells grown with (**a**) 0.75 sccm/4 μTorr and (**b**) 7.5 sccm/40 μTorr PH_3. All nanowires were grown at ~0.3 Torr total pressure at 775°C with SiH_4 flow rate/partial pressure of 3 sccm/15 mTorr on 100 nm cores. Scale bars, 500 nm. The pitch was found to decrease with low flow of PH_3 and periodic shells were not observed for high flow rates of PH_3.

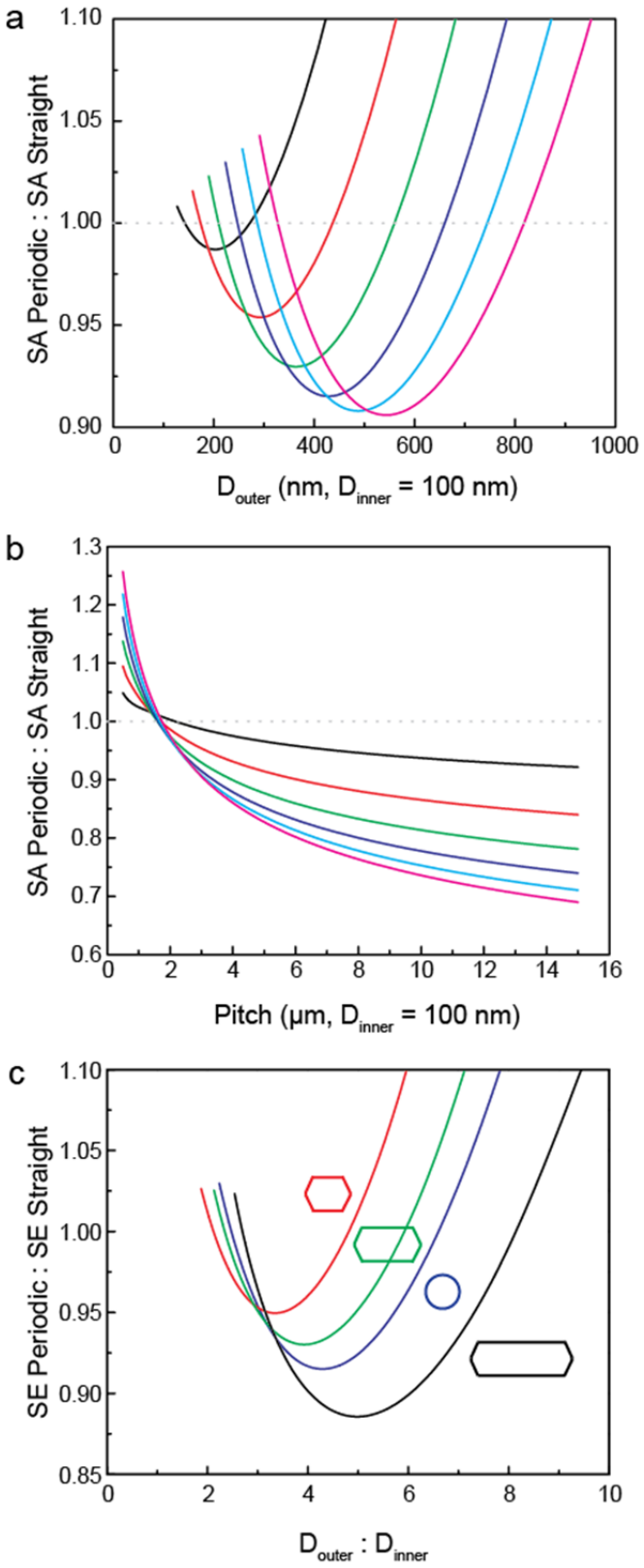

Supplementary Figure 10 | **Surface area ratio comparisons with different shell volumes. a**, Ratio of the surface area (SA) of a periodic shell nanowire to the surface area of a straight nanowire as a function of outer diameter (D_{outer}) for different shell volumes added to a 100 nm core with fixed pitch of 3 μm. **b**, The ratio of the minimum surface area of a periodic shell nanowire to the surface area of a straight nanowire as a function of pitch for different shell volumes added to a 100 nm core. For both plots, the volumes added to the periodic shell nanowires and the straight nanowires are equivalent for a given curve and inner diameters (D_{inner}) are fixed at 100 nm. Input volumes were derived from periodic shell nanowires with inner shell lengths (L_{inner}) of 1500 nm, outer shell lengths (L_{outer}) of 1500 nm, D_{inner} = 100 nm, and variable D_{outer} = 150, 200, 250, 300, 350, and 400 nm corresponding to the black, red, green, blue, cyan, and magenta curves. For reference, the blue curve in (**b**) is the same as that shown in Fig. 2c. Absolute surface area values, as shown on the right axis in Fig. 2c, are different for each plot trace, and thus specific surface areas were excluded from this multi-trace plot. **c**, Ratio of the surface energies (SE) of experimentally-observed cross section periodic shell nanowires to the surface energy of experimentally-observed cross section uniform nanowires as a function of outer diameter (D_{outer}) for the same shell volumes added to a 100 nm core as in the dark blue curve in (**a**) with fixed pitch of 3 μm. Aspect ratios for both periodic and uniform nanowires are 1 : 1.45 (red curve), 1 : 2 (green curve), and 1: 3 (black curve). For reference, the blue curve in (**c**) is the same as that shown in (**a**). In general, these plots show (1) that the surface area of a periodic shell nanowire can be lower than that of a straight nanowire of equivalent volume for a range of shell volumes, and (2) that longer pitches yield lower surface areas than shorter pitches for nanowires with equivalent volume. Incorporation of the specific geometry we observe for Si periodic shells and the surface energy densities of the prominent facets of Si periodic shell nanowires also yields lower surface energies compared to uniform diameter nanowires with equivalent volume and cross section.

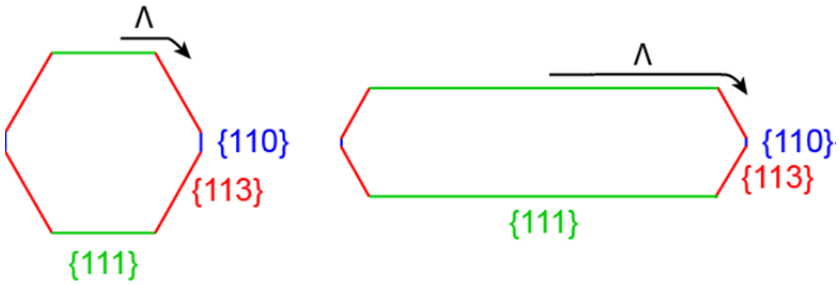

Supplementary Figure 11 | Formation of high aspect ratio periodic shell nanowires. Cross-sectional schematics of low (left) and high (right) aspect ratio Si periodic shell nanowires. The nanowires are capped by two Si(111) surfaces, four Si(113) surfaces, and two narrow Si(110) surfaces. It has been observed at conditions similar to our periodic shell growth conditions that interfacet mass-transfer of Si (i.e. net adatom surface diffusion from one facet to another) can occur provided that the diffusion lengths are much longer than the lengths of the facets[S6,S12]. Specifically, net adatom diffusion from Si(111) to the Si(113) facet occurs, elongating the (111) surface[S3,S6,S12]. Hence, it is reasonable to assert that growth at lower SiH_4 partial pressures, which will yield longer diffusion lengths[S3], Λ, will result in higher aspect ratio structures with longer (111) surfaces due to net interfacet diffusion of Si adatoms from (111) to (113).

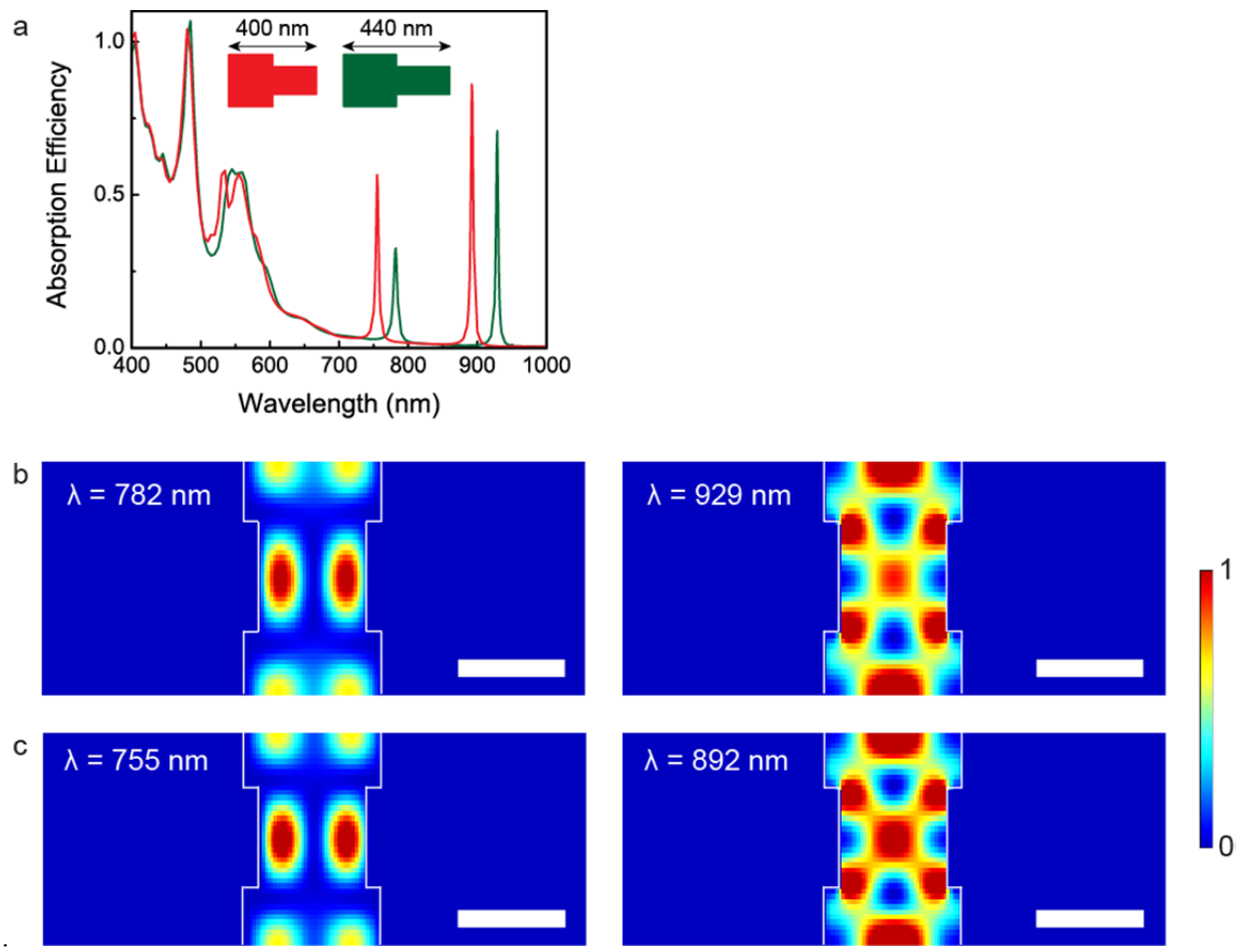

Supplementary Figure 12 | Light absorption in periodic shell nanowires with short pitches. a, FDTD simulations of the total light absorption in Si periodic shell nanowires with outer diameter of 260 nm, and inner diameter of 205 nm with pitches of 400 nm (red) and 440 nm (green). Inner and outer shell diameters are the same as in Fig. 4a and c. **b, c,** Grating mode absorption profiles from FDTD simulations corresponding to peaks in (**a**) at wavelengths >700 nm. **b**, Absorption mode profiles from green peaks located at 782 nm (left) and 929 nm (right) for the periodic shell nanowire with a pitch of 440 nm. Scale bars, 200 nm. **c,** Absorption mode profiles from red peaks located at 755 nm (left) and 892 nm (right) for the periodic shell nanowire with pitch of 400 nm. Scale bars, 200 nm. The wavelengths of grating absorption modes are determined by the pitch of periodic shell nanowires. For fixed outer and inner diameters, coupled grating modes can emerge at longer optical wavelengths when the pitch is reduced to the submicron regime.

Supplementary References

S1. Cui, Y. et al. Diameter-controlled synthesis of single-crystal silicon nanowires. *Appl. Phys. Lett.* **78**, 2214-2216 (2001).

S2. Javey, A. et al. Layer-by-layer assembly of nanowires for three-dimensional, multifunctional electronics. *Nano Lett*. **7**, 773-777 (2007).

S3. Smith, D. *Thin-Film Deposition: Principles and Practice*. (McGraw-Hill, New York, 1995).

S4. Wulff, G. Zur frage der geschwindigkeit des wachstums und der auflösung der kristallflächen. *Z. Kristall. Mineral*. **34**, 449 (1901).

S5. Lu, G.-H., Huang, M., Cuma, M, & Liu, F. Relative stability of Si surfaces: a first principles study. *Surf. Sci.* **588**, 61-70 (2005).

S6. Lim, S.-H., Song, S., Park, T.-S., Yoon, E., Lee, J.-H. Si adatom diffusion on Si (100) surface in selective epitaxial growth of Si. *J. Vac. Sci. Technol. B* **21**, 6, 2388-2392 (2003).

S7. Homma, Y., Hibino, H., Kunii, Y., Ogino, T. Transformation of surface structures on vicinal Si(111) during heating. *Surf. Sci.* **445**, 327-334 (2000).

S8. Ihle, T., Misbah, C., Pierre-Louis, O. Equilibrium step dynamics on vicinal surfaces revisited. *Phys. Rev. B* **58**, 2289-2309 (1998).

S9. Homma, Y., Hibino, H., Ogino, T., Aizawa, N. Sublimation of the Si (111) surface in ultrahigh vacuum. *Phys. Rev. B* **57**, R10237-R10240 (1997).

S10. Kempa, T. J. et al. Coaxial multishell nanowires with high-quality electronic interfaces and tunable optical cavities for ultrathin photovoltaics. *Proc. Natl. Acad. Sci. USA* **109**, 1407-1412 (2012).

S11. Kim, S.-K. et al. Tuning light absorption in core/shell silicon nanowire photovoltaic devices through morphological design. *Nano Lett*. **12**, 4971-4976 (2012).

S12. Xiang, Q. et al. Interfacet mass transport and facet evolution in selective epitaxial growth of Si by gas source molecular beam epitaxy. *J. Vac. Sci. Technol. B* **14**, 2381 (1996).